DETECTION OF HIGH-POTENTIAL GOLD, COPPER AND IRON MINERAL ZONES USING ASTER IMAGERY AND GEOCHEMICAL DATA (CASE STUDY: ARDESTAN, IRAN)

S. Mahmoudishad, A. Malian, F. Hosseinali
Dept. of Geomatic Engineering, Shahid Rajaee Teacher Training University
(S.mahmoodishad, A.malian, F.hosseinali)@srttu.edu

KEYWORDS: Independent Component Analysis (ICA), Multi-Fractal Inverse Distance Weighting (MIDW), ASTER, Remote Sensing, Geochemical Data, Ardestan

ABSTRACT:

Image processing techniques in transform domain are useful tools for combining several correlated variables into a single variable. The process of decomposing the image into uncorrelated independent components increases the accuracy and reliability of producing surface sections of the area mineral alterations. Ardestan is located in NW-SE direction of central Iranian volcanic belt that hosts many well-known porphyry copper and gold deposits. In this paper, performance of independent component analysis (ICA) has been evaluated in the identification of the anomalies associated with Cu, Au and Fe mineralization using ASTER satellite imagery and geochemical data. First of all, multi-fractal inverse distance weighted (MIDW) was developed and applied to make raster maps related to Copper (Cu), Gold (Au) and Iron (Fe) that were combined later. ICA components were then used to identify Iron oxide and hydrothermal alteration zones in the visible and near infrared (VNIR) and shortwave infrared (SWIR) subsystems of ASTER data. For this purpose, this research investigated the major absorption wavelengths of the indicator minerals. The results show that the argillic alteration zone detected by applying ICA are mostly located near the Marbin Rengan and Kacho Mesqal-Gerian faults around the geochemical anomalies. The situations of identified hydrothermal alteration zones indicate that surface sections in the study area contain porphyry copper and gold deposits. According to geochemical anomalies obtained by MIDW method, detected promising areas of Iron oxide and hydrothermal alteration zones, match precisely with the locations of Intrusions of diorite and monzonite into the igneous lithological units between marbin rengan and Kacho Mesqal-Gerian faults.

1. INTRODUCTION

Remote sensing instruments can provide detailed information on the mineralogy and geochemistry of the rock types comprising the Earth's surface, particularly for remote areas in arid or semi-arid environments that are difficult to access. Therefore remote sensing can be effective in reducing costs in large areas compared to methods such as geochemical extraction and analysis (Abulghasem et al., 2012; Zhang et al., 2007).

NW-SE trending Central Iranian Volcanic Belt is an area with high copper mineralization, therefore it has huge potential for discovering porphyry copper deposits. Ardestan that is study area in the current research is located in Central Iranian Volcanic Belt. The argillic and propylitic alterations are important signs for investigating the situation of porphyry copper and gold deposits. Different rock compositions cause the variations of outer propylitic zone in the Earth, however epidote, chlorite, and carbonate minerals are common constituents. Kaolinite, muscovite and alunite minerals reveal protrusion of middle argillic zone (Karimpour and Saadat, 1989; Mars and Rowan, 2006). Nowadays, one of the best methods for regional mapping of Iron oxide and hydrothermal alteration zones is using the Advanced Spaceborne Thermal Emission and Reflection Radiometer (ASTER). ASTER satellite images are useful for geological mapping and mineral resources exploration in vast study areas (Amer et al., 2016; Hashim et al., 2010; Pour and Hashim, 2011; Pour and Hashim, 2012; Pour et al., 2015). This sensor distinguishes the alteration zone from other minerals due to the multispectral coverage at high spatial resolution and the distinct and significant spectral features of minerals in shortwave infrared (SWIR) and thermal infrared (TIR) regions of the EM spectrum (Amer et al., 2016; Mars and Rowan, 2006; Pour and Hashim, 2011; Pour et al., 2015).

The results of studies on image processing techniques of multivariate analysis have illustrated that Independent Component Analysis (ICA) is a useful tool for combining several correlated variables into a single variable and, thus, for reducing the dimensionality of datasets into independent uncorrelated components based on covariance or correlations of variables, which represent the inter-relationships among the multi-dimensional variables (Hyvärinen et al., 2001; Pour et al., 2015; Stathaki, 2011).

Geochemical mapping is an important tool in mineral exploration (Zuo, 2011). This study collected stream sediment samples, for the determination of 46 elements, at a density of 4 samples per 10 square kilometer of the area. Statistical processing is widely applied to identify geochemical anomalies. For this purpose, the multifractal inverse distance weighted method (MIDW) supported by Geographic Information System (GIS) techniques is successfully used to

analyze geochemical data for Cu, Fe, Au and Mn elements. ICA is used to combine the concentration values of these elements. The results demonstrated the major anomalies locations in the geological map.
The results of investigation in Gangdese Belt Tibet of china used the principal component analysis (PCA) to combine the Cu, Pb, Zn and Ag concentration values that obtained by multifractal inverse distance weighted (MIDW) (Zuo, 2011). The results of recent studies have shown that ICA is an extension of PCA technique that find components which are statistically independent rather than uncorrelated; thus, it requires statistics of orders higher than the second (Lee et al., 2000). The study conducted in southern Masule in Iran using ETM+ image showed that applying ICA transformation led to the sampling program in finding unknown lithology and dikes (Gholami et al., 2012). In this paper, firstly the ICA transformation is used to map spatial distribution of Iron oxide, propylitic and argillic zones and distinguishing them from bedrocks in ASTER image to identify the section with the possibility of exploring copper deposit. Secondly, ICA are applied in raster maps of MIDW for Cu, Fe, Au and Mn geochemical elements to obtain the combination of major geochemical anomalies. Accordingly, the results of remote sensing and geochemical studies are compared with each other.

2. DATA ACQUISITION

2.1 Study area

The study area of Ardestan is located in 52° 0′ 0.00″ to 52° 30′ 0.00″ Easting, 33° 0′ 0.00″ to 33° 30′ 0.00″ Northing, NW-SE trending Central Iranian Volcanic Belt that mostly consists of volcanic pyroclastic rocks related to the Eocene and Oligocene geologic epoch in a geologic period of Paleogene. The most important intrusion in the study area is the intrusions of diorite and monzonite located in Dorojin mountain and Marbin village.
Outcrops belong to volcanic activity of post-Eocene and pre-Eocene era that are a combination of calc-alkaline and contains of rhyolite, dacite, andesite and basaltic andesite minerals. Figure 1 shows the geological conditions of this study area.

2.2 ASTER Satellite Data

The Aster image used in this study had been already pre-processed and geo-referenced to UTM zone 39N projection system with the WGS-84 datum. Crosstalk effect is an error in 4, 5 and 9 bands of ASTER images that causes the deviations from correct reflectance in false absorption features and distortion of diagnostic signatures in bands detectors on the shortwave infrared subsystem. As a result, the next processing will face the problem of identifying the wrong material (Pour and Hashim, 2012) . Crosstalk correction was applied on ASTER SWIR bands in this paper. The recommended IARR reflectance technique preferred for atmospheric correction because it does not require the prior knowledge of collected samples from the field (Pour and Hashim, 2011)

2.3 Geochemical data

The analysis of geochemical pattern that presented by the empirical density distributions is inadequate for separating the anomalies. Statistical analysis flaw for these exploration data sets is incomplete samples of geochemical landscape of a study area. Self-similarity and independence of scale in geochemical data property help to improve models of geochemical anomalies. This will not be achieved except with considering the both of spatial correlation and variability of geochemical data and the geometry and scale-independent properties of geochemical landscapes together (Carranza, 2008; Hassani Pak and Sharafodin, 2005). The fractal nature of geochemical patterns makes a relationship between fractal dimension and geochemical anomalies. The presence of geochemical anomalies increases the fractal dimension of geochemical variables. Generally, exploration data have wide range of quantities and a particular quantity rarely recurs. Therefore, for statistical analysis of geochemical raw data, it is necessary to classify them into optimum number of classes in order not to lose details. The number of classes must not be lower than $\sqrt{n}$. In this study the Sturge's Rule is used to estimate the range of classes. This rule is expressed by the following equation (Hassani Pak and Sharafodin, 2005):

$$\Delta = \frac{x_{max} - x_{\min}}{1+3.322\ \log(n)}$$

X_{max} and X_{min} are maximum and minimum of geochemical data and n is the number of data equal to the number of geochemical model cells.

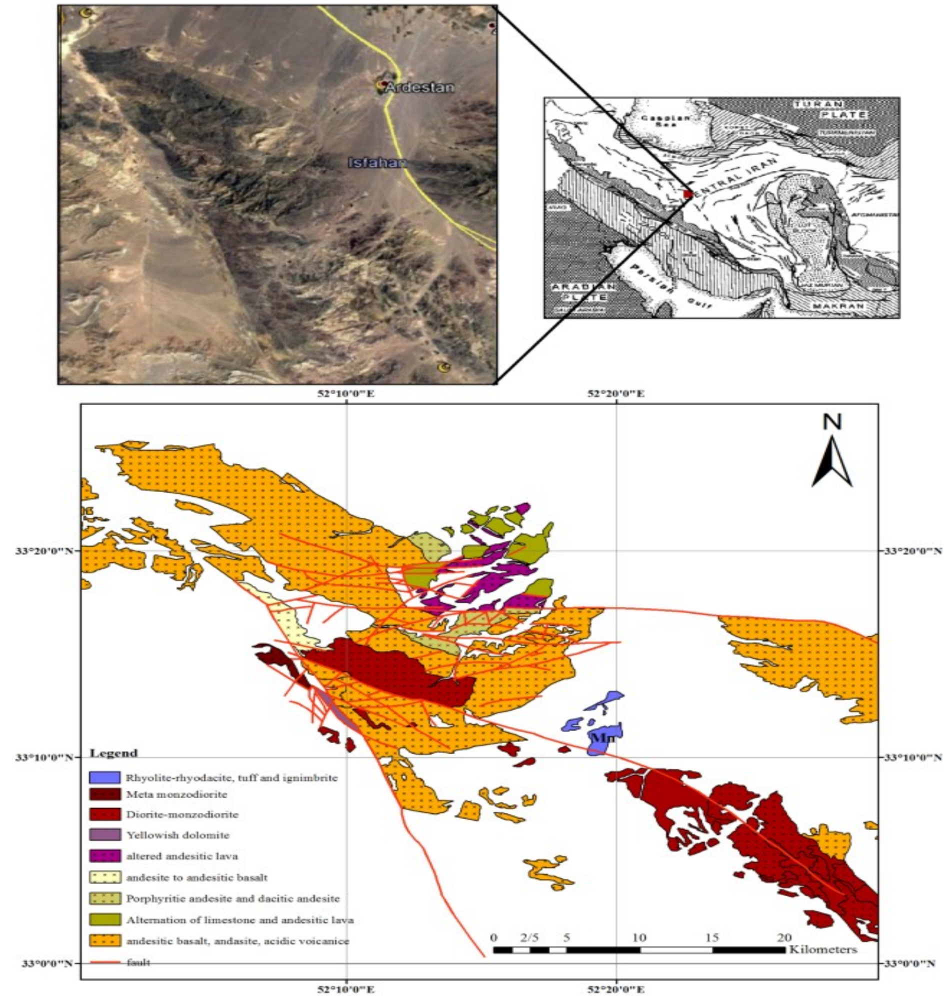

Figure 1. Geological map of Ardestan region (Produced by Geological Survey & Mineral Exploration of Iran)

3. METHOD

3.1 ICA

One of the important criteria of ICA transformation techniques is statistically independence of the transform coefficients. As a result, ICA can identify statistically independent basis vectors in linear generative model (Stathaki, 2011). This transform is based on the non-Gaussian assumption of the independent sources, and uses higher-order statistics to reveal desired features. ICA transformation can distinguish features of interest even when they occupy only a small portion of the pixels in the image that may be buried in the noisy bands of PC rotation during data whitening (Hyvärinen et al., 2001; Stathaki, 2011).

3. 2. Multifractal inverse distance weighted method

Inverse distance weighting is one of the simplest methods of weighted moving averages that is inversely proportional to the square of the distance from center of the zone of influence. While IDW implementation method is straightforward, the determination of the weights is based only on the location and ignores the variance of the values. The common disadvantage of IDW is ignoring the local properties of data. Multifractal method tries to incorporate local singularity into the basic model of IDW interpolation.

3.3. Concentration-area fractal

The concentration area fractal method can be used to separate geochemical anomalies from background. In this method, for series of values obtained from modeling geochemical samples, the values v and the areas of uni-element concentrations equal to or greater than v or the areas set of cells with equal value have multifractal properties according to the following power-law relation.

$$A(\geq v) \propto v^{-\alpha}$$

The exponent α is the slope of a straight line fitted by least squares technique through a log-log of the relation. The concentration-area relation shows multifractal properties by at least two straight lines fitted to the log-log plot. Consequently, the break in slope of straight lines can be used to distinguish different ranges of v, that mean the presence of different populations in the probability density distributions and spatial distributions of a data set of uni-element concentrations. Studies have shown that the straight line with more slope representing chemical anomalies.

3. RESULTS AND DISCUSSION

The ICA image processing technique in transform domain indicated the distribution of iron oxides in the VNIR subsystem and hydrothermal alteration mineral zones associated with porphyry copper mineralization identified and discriminated based on distinctive shortwave infrared (SWIR) properties of the ASTER data in a regional scale. Iron oxide minerals have low reflectance and higher reflectance in bands 1, 2 and band 4 of visible and near infrared of ASTER data (Pour and Hashim, 2011). Minerals associated with argillic alteration such as kaolinite, alunite and muscovite show distinctive absorption in bands 5, 6 and 7. Propylitic alteration revealed by chlorite calcite and epidote has maximum and minimum absorption in bands 5, 6 and bands 8 and 9, respectively. Iron oxides and minerals of argillic and propylitic alterations can be mapped as bright pixels in ICA2, ICA3 and ICA6, respectively.
Figure 2A showed RGB color composite of ICA 2, 3 and 6 components for demonstrating the alteration of porphyry copper deposits in ASTER data. The purple and pink color indicates the presence of iron oxide and dark blue and bright blue color indicates the argillic and propylitic alteration zones, respectively. Anomaly of Iron oxide and hydrothermal alteration zones in bands 2, 3 and 6, have been separated with thresholds 1.7, -1.3 and 1.3, respectively (Figure 2B).
According to the geochemical reports used in this paper, among 959 geochemical samples used for identification of 45 types of minerals, , only Cu, Fe, Au and Mn are studied in the current research at a density of 4 samples per 10 km^2 in 2582.652 km^2 of the desired area. Figure 3 depicts the distribution of points in the region. These choices are due to the importance of minerals in identifying areas with high mineral potential. The statistical parameters of non-normal data distributions for these elements are indicated in table 1.
In this study, there are three steps in analyzing geochemical data for each element.

1. Applying IDW method to generate a network of interpolated values for the entire region.
2. Classifying geochemical data obtained by IDW model to draw a logarithmic curve of concentration-area.
3. Generating MIDW model based on variation of the fractal dimension obtained from the logarithmic curve.

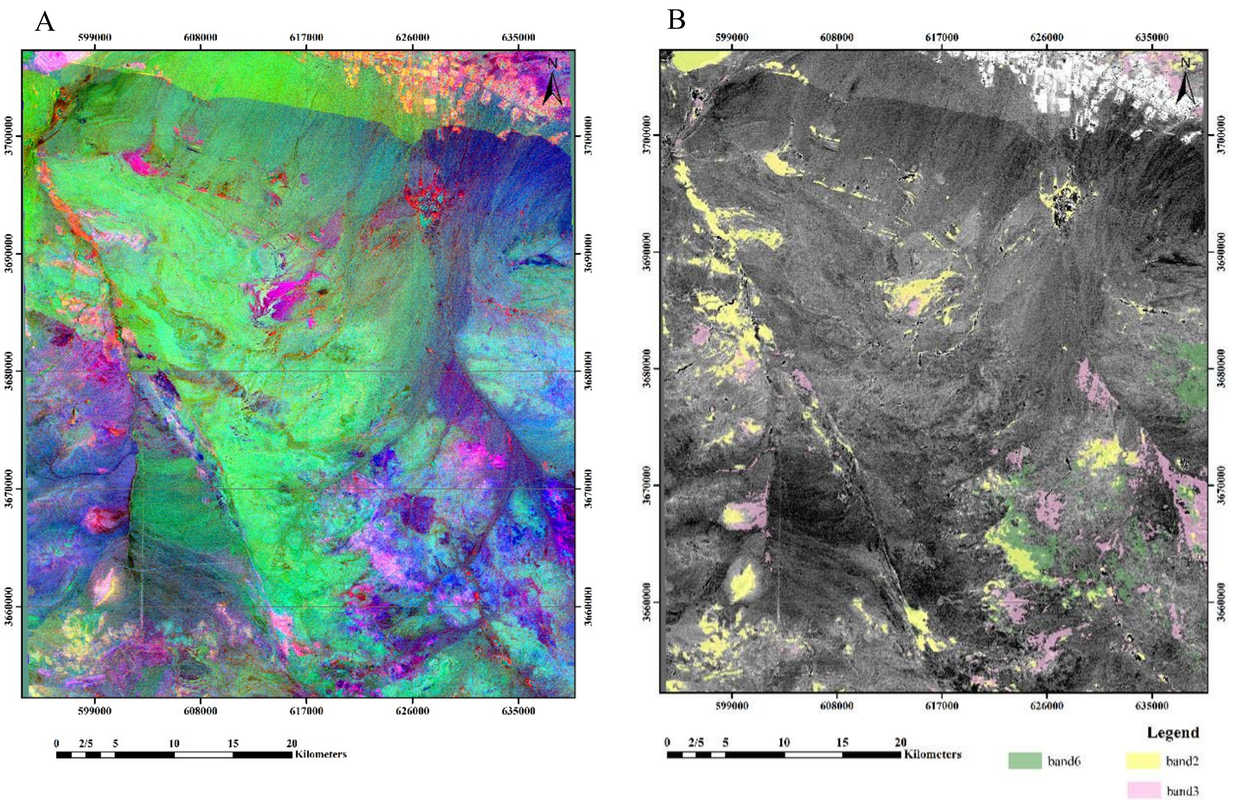

Figure 2. A) RGB color composite of ICA 2, 3 and 6 components for demonstrating Iron oxide and hydrothermal alteration zones. B) ICA band 2,3 and 6 with anomalies have been isolated by applying the thresholds to the related bands (ICA 2, 3 and 6). These figures are showed in UTM zone 39N projection with the WGS-84 datum.

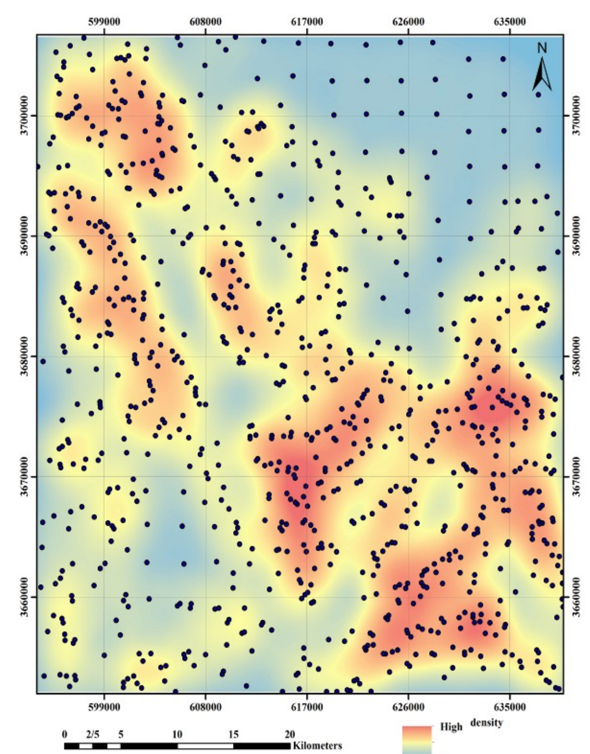

Figure 3. Distribution of situation of geochemical samples in the study area (Ardestan)

Table 1. Descriptive statistics of stream sediment geochemical samples.

	Cu	**Fe**	**Au**	**Pb**
Number of samples	959	959	959	959
Mean	33.64	4.224	0.001	1008.43
Std. deviation	21.761	0.45	0.0004	143.126
Median	31.9	4.21	0.0009	992
Mode	32.8	4.45	0.0007	953
Range	264	8.78	0.0172	3895
Variance	473.54112	0.2025	1.60E-07	20484.93
Skewness	7.014	0.769	9.511	5.51
Maximum	277.1	10.54	0.0174	4414
Minimum	13.1	1.76	0.00016	519
Threshold	91.93	5.123	0.0019	67.558

The areas enclosed with the thresholds are obtained with MIDW. The threshold occurs in variation of the fractal dimension. Figure 4 shows the raster maps of the distributions of Cu, Fe, Au, and Mn created by the MIDW interpolation in Arc GIS and MATLAB software. The threshold and range of anomaly for each element are consistent with the results of statistical analysis.

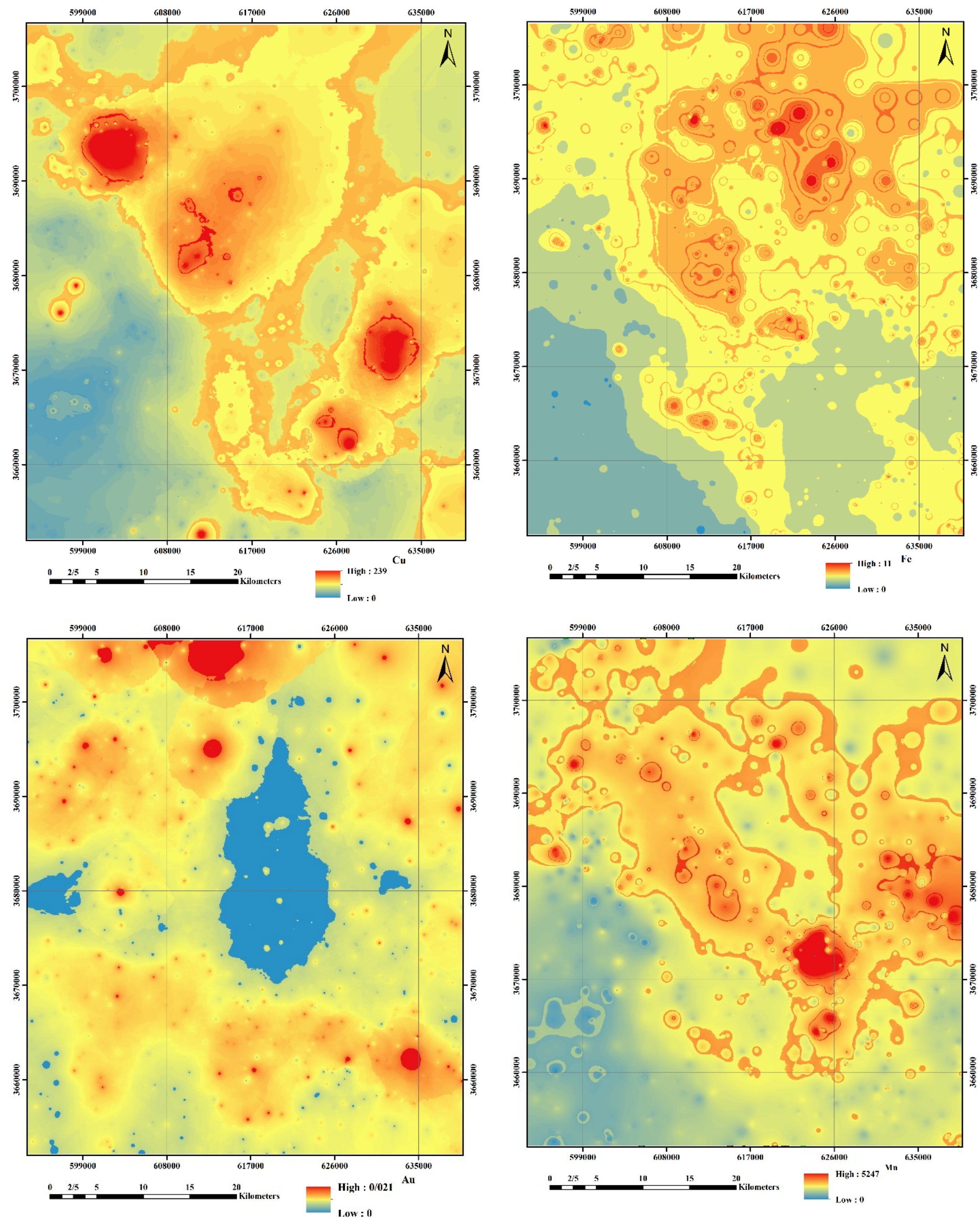

Figure 4. The raster maps of the distributions of Cu, Fe, Au, and Mn created by MIDW

The value of Cu, Fe, Mn and Au samples are classified into 24, 22, 22, and 24 ranges, respectively. The log-log plot of these elements indicates the significant fractal dimension in ranges [33.69 , 173.69], [5.161 , 7.960], [1127.2 , 1999.9] and [0.0027 , 0.077] (green line in log-log plot of Figure 5). These ranges of mineral anomalies for Cu, Fe and Mn are divided into smaller classes due to the large range of possible anomalies.

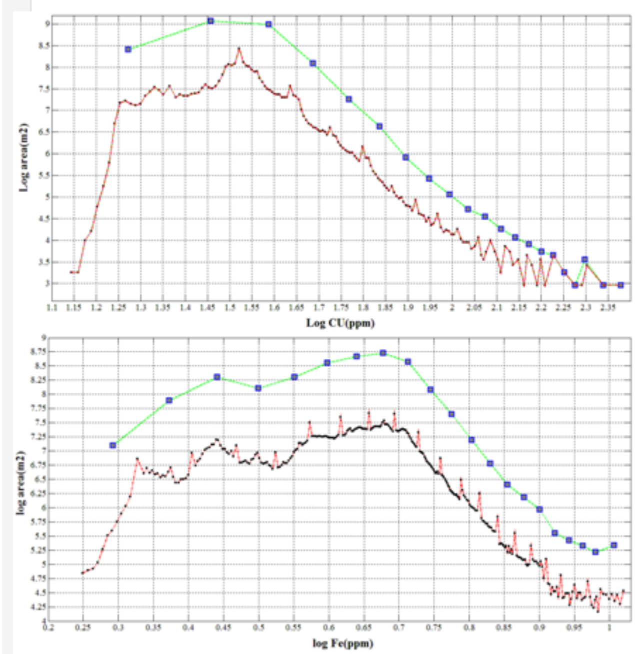

Figure 5. log–log plots (concentration-area) of Cu, Au, Fe and Mn

As shown in the Figure 5, the log-log plot of new classes with red color shows a fractal behavior. The observed oscillations in the red curve indicates the presence of multiple populations in the large range of possible anomaly with the maximum variations of slope in the curve, that can be created due to influence of various geological events or processes.

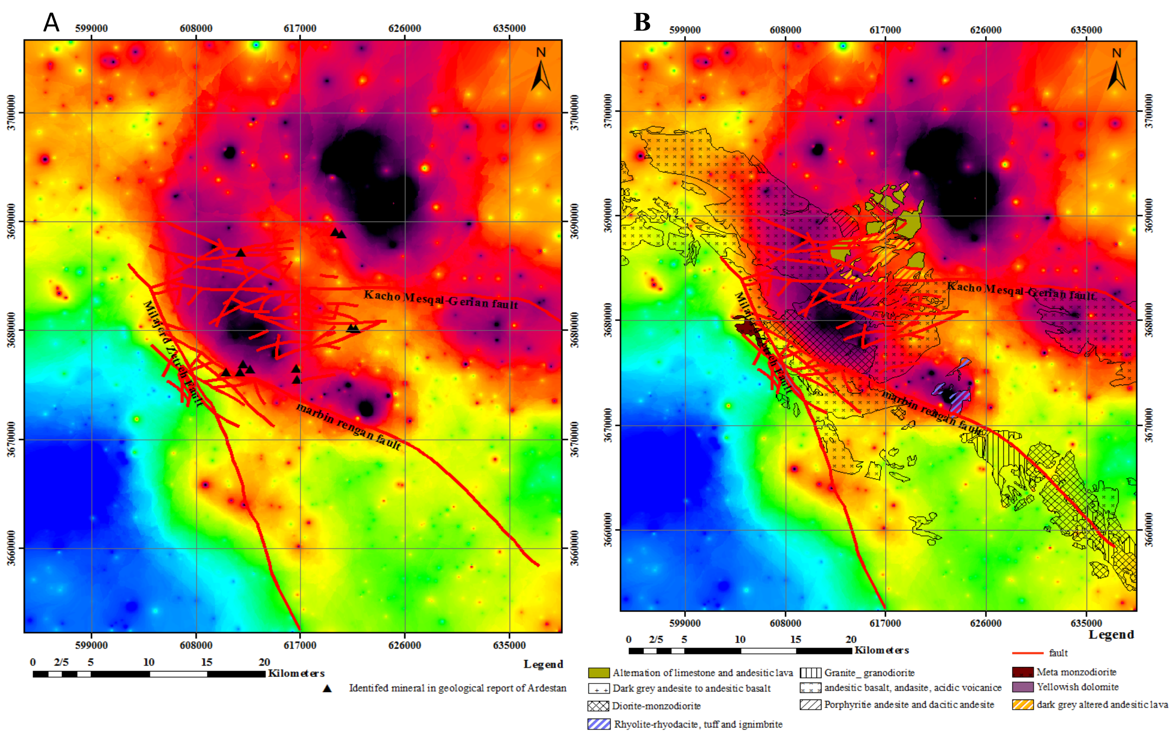

Figure 6. A) ICA1 mage with maximum eigenvalue has correlation with Cu, Au and Mn MIDW images greater than other components. B) The appearance of the anomalies match with the position of the main faults and igneous rocks of the study area.

The first independent component accounts for 73.6% of the total variance in the multivariate data. The eigenvectors show that Cu, Au and Mn are the most important contributors to the first independent component. The anomaly map (Figure 6A) shows an NW-SE trend that is located in central part of the Ardestan matching precisely with the location of mineralized zones of the region referred in geological report. The limited area of anomaly obtained by ICA1 method shows that values of integrated anomalies of Cu, Au, Fe and Mn occur in proximity and orientation of fault in intrusive rocks near igneous units (Figure 6B).

4. CONCLUSION

Recent geological studies suggest that Central Iranian Volcanic Belt hosts many well-known porphyry copper deposits. In this paper, the ICA transformation technique and spectral features of minerals were used for the Iron oxide and argillic and propylitic alteration zones mapping. The exploration indicator minerals from image processing of ASTER data are located aligned with the direction of the faults and surrounded by the igneous units. The results of Multifractal interpolation of Cu, Au, Fe and Mn associated with porphyry copper and gold deposits show the location of geochemical anomalies between marbin Rengan and Kacho Mesqal-Gerian faults in Ardestan region. Finally, the following conclusions are obtained from remote sensing data processing and geochemical analysis:

1. The ICA method is a useful tool for integrating multi-element concentration values for exploration the geochemical anomaly related to investigated mineral.
2. The ICA method can be assumed as an applicable and efficient method for extraction of mineral alteration from igneous lithological units.
3. The integrated anomalies of Cu, Au, Fe and Mn occurring between Marbin Rengan and Kacho Mesqal-Gerian faults in the intrusive rocks of the NW-SE trend center part of Ardestan, should be further investigated in the next phase of mineral exploration.
4. Processing of remote sensing imageries can be used to identify the location of zones with high potential of porphyry copper deposits. It is useful from an economic point of view to identify the appropriate area for geochemical studies.

REFERENCES

Abulghasem, Y.A., Akhir, J.B.M., Hassan, W.F.W., Samsudin, A.R., Youshah, B.M., 2012. The use of remote sensing technology in geological investigation and mineral detection in Wadi shati, Libya. Electronic Journal of Geotechnical Engineering 17, pp. 1279-1291.

Amer, R., El Mezayen, A., Hasanein, M., 2016. ASTER spectral analysis for alteration minerals associated with gold mineralization. Ore Geology Reviews 75, pp. 239-251.

Carranza, E.J.M., 2008. Geochemical anomaly and mineral prospectivity mapping in GIS. Elsevier, pp. 86.

Gholami, R., Moradzadeh, A., Yousefi, M., 2012. Assessing the performance of independent component analysis in remote sensing data processing. Journal of the Indian Society of Remote Sensing 40, pp. 577-588.

Hashim, M., Pour, A.B., Marghany, M., 2010. Characterization of ASTER data for mineral exploration. international remote sensing & gis conference and exhibition.

Hassani Pak, A., Sharafodin, M., 2005. Exploration data analysis. Tehran University, Iran (in Persian), pp. 446-448.

Hassani Pak, A., Sharafodin, M., 2005. Exploration data analysis. Tehran University, Iran (in Persian), pp. 6-12.

Hyvärinen, A., Karhunen, J., Oja, E., 2001. Independent Component Analysis. Finland Neural Networks, 13(4-5), pp.411-430.

Karimpour, M., Saadat, S., 1989. Applied economic geology. Javid Publication, Mashhad, Iran, pp. 179-197.

Lee, T.-W., Girolami, M., Bell, A.J., Sejnowski, T.J., 2000. A unifying information-theoretic framework for independent component analysis. Computers & Mathematics with Applications 39, pp. 1-21.

Mars, J.C., Rowan, L.C., 2006. Regional mapping of phyllic-and argillic-altered rocks in the Zagros magmatic arc, Iran, using Advanced Spaceborne Thermal Emission and Reflection Radiometer (ASTER) data and logical operator algorithms. Geosphere 2, pp. 161-186.

Pour, A.B., Hashim, M., 2011. Identification of hydrothermal alteration minerals for exploring of porphyry copper deposit using ASTER data, SE Iran. Journal of Asian Earth Sciences 42, pp. 1309-1323.

Pour, A.B., Hashim, M., 2012. The application of ASTER remote sensing data to porphyry copper and epithermal gold deposits. Ore Geology Reviews 44, pp. 1-9.

Pour, A.B., Hashim, M., Pournamdari, M., 2015. Chromitite Prospecting Using Landsat TM and Aster Remote Sensing Data. ISPRS Annals of the Photogrammetry, Remote Sensing and Spatial Information Sciences 2, pp. 99.

Stathaki, T., 2011. Image fusion: algorithms and applications. Academic Press, pp. 90-91.
Zhang, X., Pazner, M., Duke, N., 2007. Lithologic and mineral information extraction for gold exploration using ASTER data in the south Chocolate Mountains (California). ISPRS Journal of Photogrammetry and Remote Sensing 62, pp. 271-282.
Zuo, R., 2011. Identifying geochemical anomalies associated with Cu and Pb–Zn skarn mineralization using principal component analysis and spectrum–area fractal modeling in the Gangdese Belt, Tibet (China). Journal of Geochemical Exploration 111, pp. 13-22.